substance: $FeSb_2$
property: physical properties

Energy level scheme is similar to that of $FeAs_2$ (Fig. 1).

The observed Schottky anomaly (excess heat capacity, Fig. 9) can be interpreted by assuming that the [4]b band is in fact split, so that the highest occupied [2]b band is succeeded by a [2]$a_{\|}$ and a [4]σ^* band at E_1 and E_2, respectively, in Goodenoughs picture. E_1/hc = 300 cm^{-1} (E_1 = 0.037 eV), E_2/hc = 500 cm^{-1} (E_2 = 0.062 eV) [77G].

energy gap and activation energy

(all values from $\log \rho \propto E_g/2kT$)

$E_{g,th}$	≈ 7 eV	polycrystalline, T = 550...800 K	60D
E_A	≈ 0.05 eV	sintered sample, T = 500...700 K	59H
	≈ 0.03 eV	sintered at T = 873 K, T = 80...160K	65J
	0.033 eV	single crystal, T = 50...300 K	72S, 72F
	≈ 0.02 eV	pressed pellets, T = 80...300 K	80Y

Debye temperature

Θ_D	327 K	from Mössbauer isomer shift	72S
		270...560 K	

electrical resistivity: Figs. 3...5, anisotropy of the resistivity: Fig. 3, anisotropy of the Hall constant: Fig. 6.

thermoelectric power

S	+ 30 μV K^{-1}	T = 295 K	polycrystal and single crystal of unknown orientation; for temperature dependence in the range 77...400 K, see Fig. 2	60D, 72F

magnetic susceptibility

χ_m	522·10^{-6} cm^3 mol^{-1}	T = 300 K	measured on sintered material,	80Y
	8·10^{-6} cm^3 mol^{-1}	T = 77 K	annealed at 873 K; χ in CGS-emu	

For temperature dependence in the range 77...550 K, see Fig. 7.

peritectic temperature

T_{perit}	1005 K		58H
	1011 K		72M
	1021 K	from heat capacity	69S, 77G
	1018 K		77K

The statement [72F, 72R] that $FeSb_2$ decomposes under vacuum towards 600 K into FeSb + Sb was refuted by [77G].

heat capacity: C_p in the range 100...700 K: Fig. 8, Schottky anomaly: Fig. 9.

Brinell hardness

H_B	200 kg mm^{-2}	60K

unit-cell dimensions $a(T)$, $b(T)$, $c(T)$ fairly linear in T [77K].

volume expansion coefficient

β	$6.1 \cdot 10^{-5}$ K^{-1}	T = 300 K	from graphical representation; unit-cell volume linear in T up to ≈ 1000 K	77K

Comparative tables on structural data of transition metal dipnictides:

structure, chemical bond: see document ,

crystallographical data of compounds with octahedrally coordinated cations, see document ,

interatomic distances in marcasite- and loellingite-type compounds, see document .

References:

58H Hansen, M., Anderko, K.: Constitution of Binary Alloys, McGraw Hill, New York, second ed. 1958, 1138.

59H Hulliger, F.: Helv. Phys. Acta 32 (1959) 615.

60D Dudkin, L. D., Vaidanich, V. I.: Fiz. Tverd. Tela 2 (1960) 1526; translation: Sov. Phys. Solid State 2 (1960) 1384.

60K Kuz'min, R. N., Zhuravlev, N. N., Losievskaya, S. A.: Kristallografiya 4 (1960) 218; translation: Sov. Phys. Cryst. 4 (1960) 202.

65J Johnston, W. D., Miller, R. C., Damon, D. H.: J. Less-Common Met. 8 (1965) 272.

69S Shunk, F. A.: Constitution of Binary Alloys, Second Supplement. McGraw-Hill, New York 1969.

72F Fan, A. K. L., Rosenthal, G. H., McKinzie, H. L., Wold, A.: J. Solid State Chem. 5 (1972) 136.

72G Goodenough, J. B.: J. Solid State Chem. 5 (1972) 144.

72M Maier, J., Wachtel, F.: Z. Metallkde. 63 (1972) 411.

72R Rosenthal, G., Kershaw, R., Wold, A.: Mat. Res. Bull. 7 (1972) 479.

72S Steger, J., Kostiner, F.: J. Solid State Chem. 5 (1972) 131.

74K Kjekshus, A., Rakke, T.: Acta Chem. Scand. A28 (1974) 1001.

77G Grenvold, F., Highe, A. J., Westrum, Jr., E. F.: J. Chem. Thermodyn. 9 (1977) 773.

77K Kjekshus, A., Rakke, T.: Acta Chem. Scand. A31 (1977) 517.

80Y Yamaguchi, G., Shimada, M., Koizumi, M., Kanamaru, F.: J. Solid State Chem. 34 (1980) 241.

Fig. 1.

$FeAs_2$. One-electron energy levels for the valence electrons in loellingite [72F, 72G].

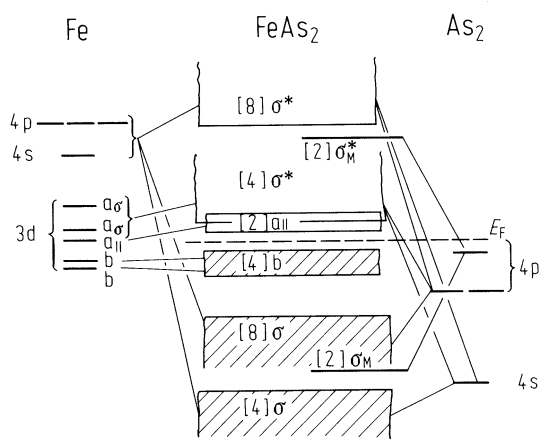

Fig. 2.

$FeAs_2$, $FeSb_2$, $OsSb_{1.95}Te_{0.05}$. Seebeck coefficient vs. temperature [65J]. $FeAs_2$: polycrystalline natural sample containing traces of calcite; $FeSb_2$ and $OsSb_{1.95}Te_{0.05}$: pressed samples sintered at 873 K and 973 K, respectively.

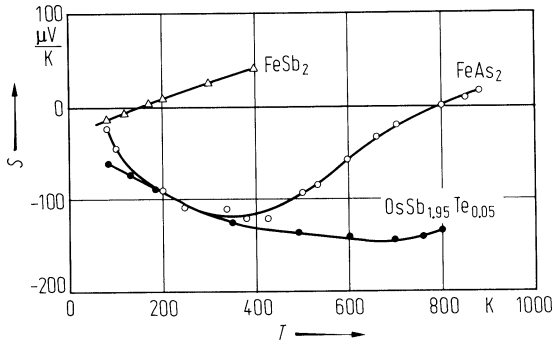

Fig. 3.

$FeSb_2$. Electrical resistivity vs. reciprocal temperature of an n-type single crystal [72F]. Triangles: measurement made in the (*a*,*b*) plane; circles: measurement made in the (*a*,*c*) or in the (*b*,*c*) plane.

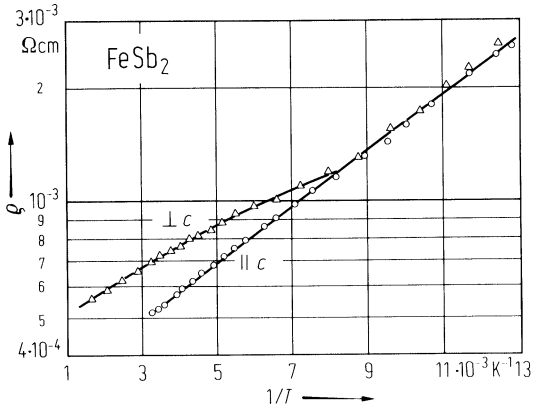

Fig. 4.

$FeSb_2$ and $OsSb_{1.95}Te_{0.05}$. Electrical resistivity vs. reciprocal temperature [65J]. Sintered samples. $FeSb_2$: *1* [60D], *2* [59H], *3* [65J].

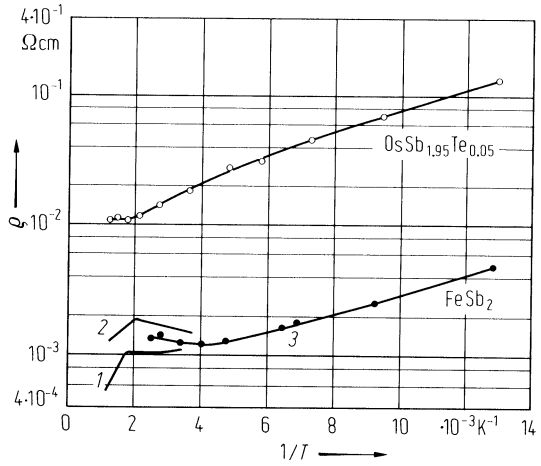

Fig. 5.

$FeSb_{2-x}Te_x$. Electrical resistivity vs. reciprocal temperature [80Y]. Compounds with x = 0.8, 1 and 1.2 crystallize in the monoclinic arsenopyrite structure.

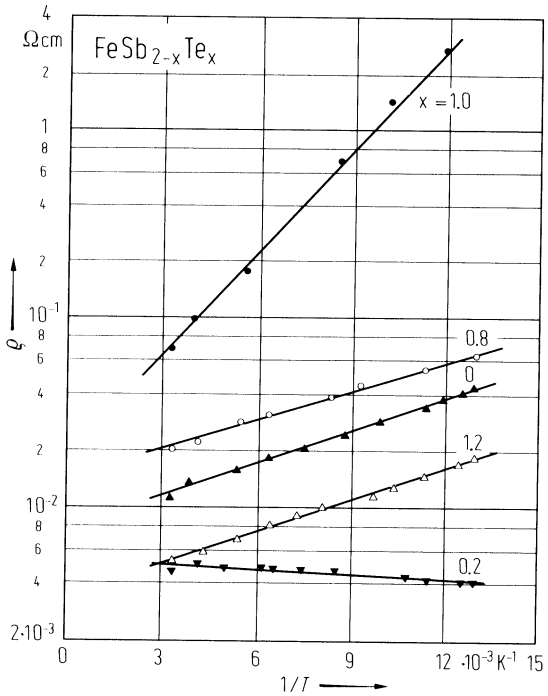

Fig. 6.

$FeSb_2$. Hall coefficient vs. reciprocal temperature [72F]. Open circles: Measurement made with the magnetic field perpendicular to the (*a*,*b*) plane; full circles: magnetic field parallel to the (*a*,*b*) plane.

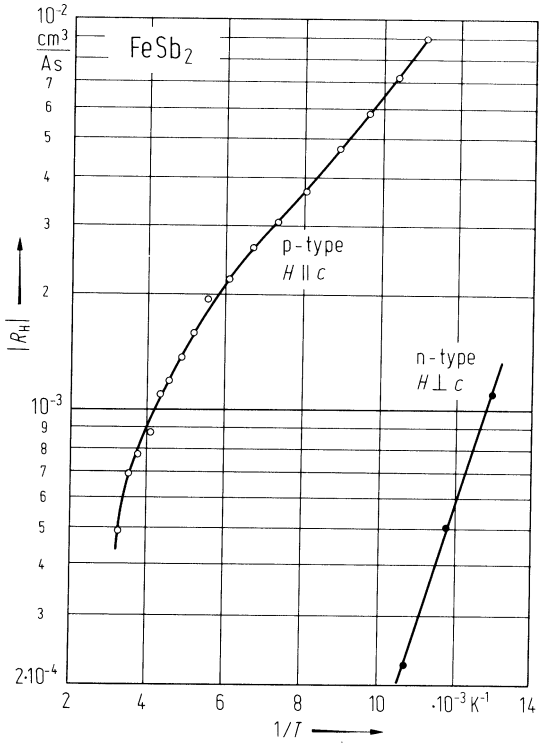

Fig. 7.

$FeSb_2$. Magnetic susceptibility vs. temperature of non-oriented single crystals grown by a chlorine transport reaction [72F]. Full circles represent the data of [80Y], see table. χ_m in CGS-emu.

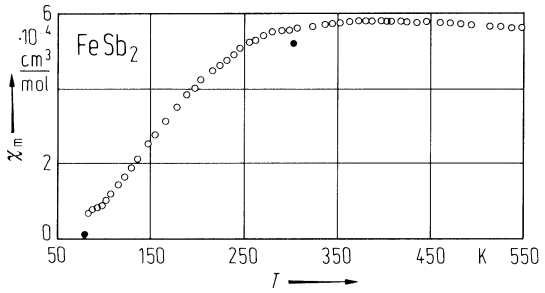

Fig. 8.

$FeSb_2$. Molar heat capacity vs. temperature [77G]; 190 g sample. For comparison the experimental and (above 350 K) extrapolated heat capacity of $FeTe_2$ is added (broken curve).

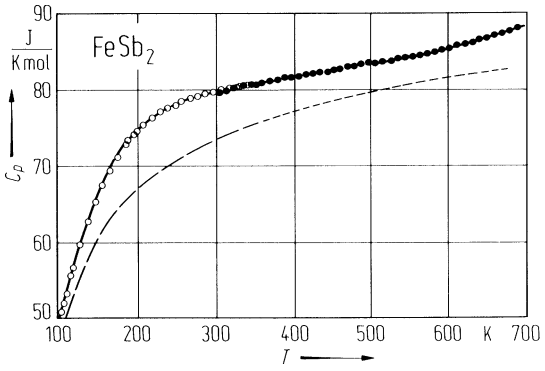

Fig. 9.

$FeSb_2$. Excess molar heat capacity vs. temperature [77G]. Broken curve: Calculated Schottky anomaly for electron excitations from a ground level to a first level at E_1/hc = 300 cm^{-1} and to a second level E_2/hc = 500 cm^{-1}, with the corresponding degeneracies $g_0 : g_1 : g_2$ = 1: 1: 2.